Korean J. Chem. Eng., **28**(4), 1035-1041 (2011)
DOI: 10.1007/s11814-010-0474-2

Removal of melanoidin from molasses spent wash using fly ash-clay adsorbents

Ali Ramezani*, Ghasem Najafpour Darzi,†, and Maedeh Mohammadi****

*Faculty of Chemical Engineering, Islamic Azad University of Shahrood Branch, Shahrood, Iran
**Faculty of Chemical Engineering, Noushirvani University of Technology, Babol, Iran
(*Received 14 February 2010 • accepted 8 November 2010*)

Abstract−Removal of melanoidin pigment from molasses spent wash was investigated using a new adsorbent. Solid adsorbents were fabricated from charcoal fly ash and clay. The effect of various molasses concentration (6 to 12 g/*l*) on removal efficiency was studied. The obtained results revealed that maximum removal efficiency of 82% was achieved at the molasses concentration of 6 g/*l* and contact time of 7 h. The saturated porous adsorbents were regenerated and reused to conduct similar experiments. The achieved data showed that more than 90% of the capacity of the fresh adsorbent was recovered after regeneration. Various adsorption isotherms of Langmuir, Freundlich, Temkin and Harkins-Jura were applied to interpret the obtained experimental data. The obtained results revealed that the sorption data were well described by the Harkins-Jura model. Also, various kinetic models of pseudo-first order, pseudo-second order, Elovich and intra-particle diffusion were used to predict the characteristic parameters which are useful in process design. It was concluded that the best fit was obtained with pseudo-second order kinetic model at low molasses concentrations.

Key words: Clay, Fly Ash, Isotherms, Kinetics, Melanoidins, Molasses

INTRODUCTION

Depletion of fossil energy resources and deterioration of the environment are two major concerns of mankind. These issues remind us of the need to find alternative fuel resources which could be renewable, sustainable and count for eco-friendly fuels. Therefore, in developed countries there is a growing trend towards the use of biomass-based energies. These technologies, which use waste or plant matter to produce energy, emit less greenhouse gas than fossil fuels and are cost-wise competitive with conventional energy resources [1,2].

Liquid biofuel, especially bioethanol, is one of the alternatives with the potential to be replaced with fossil fuels. Bioethanol can be produced from various feedstocks such as sugarcane residues, corn stoves, wood wastes and agricultural residues [3]. Among all these resources, sugar-based residues contain fermentable sugar and are appropriate for ethanol production; whereas, the other resources require additional pretreatment processes to become fermentable sugar [4].

Molasses is one of the byproducts of the sugar production process and is the final residue from the sugar crystallization unit. It is used as a carbon source for animal feed and biofertilizer. Molasses is also the most common feedstock for fermentation industries such as ethanol and backer's yeast production. It has a high content of sugar and is locally available in low cost [5-7].

The major problem associated with the molasses industry is the production of large quantities of brown-colored effluents known as spent wash. It has been reported that molasses spent wash in alcohol fermentation is nearly 15 times of the total amount of alcohol produced [8]. Disposal of such huge quantity of waste stream without further treatment can cause serious environmental damages. The effluent streams of these industries are extremely colored and have high organic load. The spent wash is characterized as a waste effluent having very high chemical oxygen demand (COD) (65,000-130,000 mg/*l*) and biochemical oxygen demand (BOD_5) (30,000-96,000 mg/*l*), acidic pH (4-5), bad smell and dark brown color [9]. The main colored compounds that are developed during sugar processing can be categorized into three major groups of melanins, melanoidins and caramels [10].

Melanoidins widely originate from molasses-based distilleries and fermentation industries. Formation of melanoidins involves a set of chemical reactions between amino compounds and carbohydrates during the Maillard reaction [11]. Melanoidin has the empirical formula of $C_{17\text{-}18}H_{26\text{-}27}O_{10}N$ with a molecular weight in the range of 5,000 to 40,000 [12]. Melanoidin has commercial and nutritional significance as it serves the color and flavor of the foods, which are the key factors to attracting consumers. But, investigations have revealed some harmful effects of melanoidins as mutagenic, carcinogenic and cytotoxic effects [11]. Therefore, discharge of the highly colored spent wash, which is enriched with melanoidin, is a great threat to the environment. The dark brown color of these effluents prevents sunlight and oxygen to penetrate into aquatic systems such as rivers, lakes and lagoons. Disposal of such waste streams into the soil reduces its alkalinity and manganese content. It also inhibits seed evolution and destroys vegetation [13,14].

Decolorization of molasses spent wash by physical, chemical and biological methods has been investigated by a number of researchers [5,12,15-19]. Adsorption as a physical treatment technique has proven to be effective for wastewater treatment. Although adsorption may be a costly method, utilizing low cost materials as adsorbent makes the adsorption process to be cost effective [12,15]. Fly ash and clay have been found as potential and low cost adsorbents to remove color from waste streams. Clay is a natural scavenger of

†To whom correspondence should be addressed.
E-mail: najafpour@nit.ac.ir

water pollutants and fly ash is a waste material, originating in significant amounts in combustion process. Currently, annual worldwide production of coal ash is estimated to be 700 million tons, from which at least 70% is fly ash [12]. Although part of the fly ash is used in applications such as light concrete preparation, large quantities are still not used and disposed. The large amount of fly ash discarded in coal-fired power stations can be utilized as a potential adsorbent for color removal [12,15,20].

The aim of the present research was to investigate the decolorization of molasses spent wash by using a novel adsorbent. The adsorbent was fabricated from a mixture of charcoal fly ash and clay. The performance of the fabricated adsorbent was evaluated in a series of batch experiments. Various adsorption isotherms and kinetic models were implemented to interpret the experimental data. The coefficients and important parameters of these models were also calculated.

MATERIALS AND METHODS

1. Preparation of the Adsorbent

Molasses was provided from a local sugar factory, Fariman, Iran. It was a dark brown and dense liquor with sugar concentration of 315 g/*l*. DNS method was applied to determine the sugar concentration of the molasses before and after the decolorization process [21].

Fly ash was locally obtained from Tonekabon, Iran. It was supplied from combustion of wood-wastes. Clay was provided from a ceramic industry, Sophal Tabarestan, Neka, Iran. A solid mixture of fly ash and clay with proportions of 60 and 40 wt% was prepared. The mixture was blended thoroughly and uniformly. In the preparation process of the granulated adsorbents, 10 ml of distillated water and 10 ml of 8 wt% polyvinyl alcohol (Merck, Germany) were added to 8 g of uniformly mixed solid adsorbent. The paste material was pelletized, air-dried and placed in a furnace (Nobertherm, Germany) and heated to 600 ºC for 2 h. The porous and calcined solid pellets were used in batch experiments. Fig. 1 shows the SEM micrograph of the fabricated adsorbent.

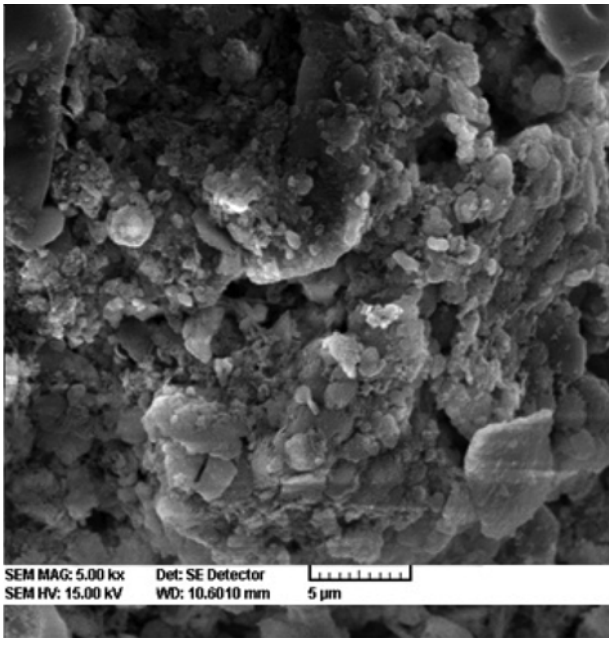

Fig. 1. SEM micrograph of the fabricated adsorbent.

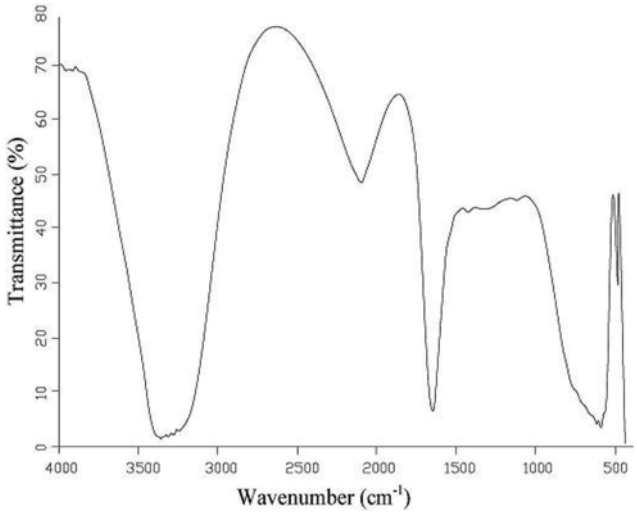

Fig. 2. FTIR spectrum of the fly ash-clay adsorbent.

To determine the surface functional group of the adsorbent, a Fourier transform infrared (FTIR) spectrum was recorded over the frequency range of 4,000 to 400 cm^{-1} using a spectrometer (Bruker, Model Vector 22, Germany). Fig. 2 shows the FTIR spectrum of the fly ash-clay adsorbent. The FTIR spectrum of the adsorbent indicated the presence of several functional groups. The presence of a strong absorption band at 3,300 cm^{-1} confirmed the presence of dominant hydroxyl group (–OH). The carbonyl functional group (C=O) was found at wavelength of 1,640 cm^{-1}. The peaks at wavelength of 2150 cm^{-1} represented carboxyl (-COO) functional group [22]. All of these surface functional groups of the fabricated adsorbent can interact with the molasses molecule.

2. Batch Experiments

To obtain the equilibrium concentration of the adsorbate, batch experiments were conducted in a series of Erlenmeyer flasks (250 ml). Each flask contained 5 g of the adsorbent and 100 ml of 10 g/*l* molasses solution (10 g molasses was diluted in 1,000 ml of distilled water). All the flasks were kept at the same condition. They were placed in a shaker (Stuart, UK) which was set at 190 rpm to ensure sufficient mixing and effective mass transfer. A similar procedure was followed for another set of Erlenmeyer flasks containing the same molasses solution without the adsorbent as blank. For a time interval of 60 min, flasks were removed from the shaker and the final concentrations of pigments in the solution were analyzed. To determine the equilibrium concentration, the adsorption experiment was prolonged to 20 h. However, it was observed that a contact time of 7 h was enough to achieve equilibrium as the molasses removal efficiency was almost constant after this contact time. The molasses concentration was determined with a spectrophotometer (Unico, 2100 series, USA). Maximum absorbance was found to be at the wavelength of 664 nm for molasses. A calibration curve was developed for a range of molasses solutions with defined concentrations. The final concentration of the samples was determined by using the calibration curve. Similar experiments were conducted with various molasses concentrations of 6, 8 and 12 g/*l* to determine the equilibrium concentrations. The amount of molasses adsorbed per mass

Table 1. The linearized form of various applied adsorption isotherms

Isotherm model	Linear equation
Langmuir	$\frac{C_e}{q_e}=\frac{1}{K_L q_{max}}+\frac{C_e}{q_{max}}$
Freundlich	$\log q_e=\log K_F+\frac{1}{n}\log C_e$
Temkin	$q_e=B_1 \ln K_T+B_1 \ln C_e$
Harkins-Jura	$\left(\frac{1}{q_e^2}\right)=\left(\frac{B_2}{A}\right)-\left(\frac{1}{A}\right)\log C_e$

Table 2. The linearized form of various applied kinetic models

Kinetic model	Linear equation
Pseudo-second order	$\log(q_e-q)=\log q_e-\frac{k_1}{2.303}t$
Pseudo-second order	$\frac{t}{q_t}=\frac{1}{kq_e^2}+\frac{t}{q_e}$
Elovich	$q=\frac{1}{\beta}\ln(\alpha\cdot\beta)+\frac{1}{\beta}\ln t$
Intra-particle diffusion	$q=f\left(\frac{Dt}{r_p^2}\right)^{1/2}=K_i t^{1/2}+I$

of the adsorbent was calculated based on the following equation:

$$q=\frac{(C_0-C)\cdot V}{W} \quad (1)$$

3. Regeneration of the Adsorbents

To regenerate the saturated adsorbents, the used adsorbents were heat treated and baked in the furnace at 600 ºC for 1 h in the presence of air. Similar batch experiments were conducted with the regenerated adsorbents. The molasses removal efficiency of the fresh and regenerated adsorbents was compared.

4. Adsorption Isotherms and Kinetic Models

Various adsorption isotherms of Langmuir [23], Freundlich [23], Temkin [24] and Harkins-Jura [24] were used in this study to interpret the obtained experimental data. The linearized form of various adsorption isotherms are summarized in Table 1.

The controlling mechanism of the adsorption process was investigated by fitting pseudo-first order [25], pseudo-second order [25], Elovich [23] and intra-particle diffusion [25] kinetic models to the experimental data. Various applied kinetic models are tabulated in the linearized form in Table 2.

RESULTS AND DISCUSSIONS

1. Effect of Initial Molasses Concentration on Removal Efficiency and Adsorption Capacity

To evaluate the effect of molasses concentration on removal efficiency, various concentrations of 6, 8, 10 and 12 g/*l* were examined. The amount of molasses removed from the solution was calculated based on the following equation:

$$\text{Molasses removal efficiency } (\%)=\left(\frac{C_o-C_t}{C_o}\right)\times 100 \quad (2)$$

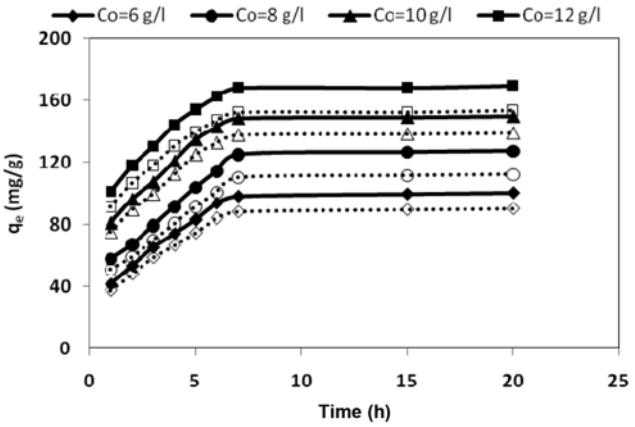

Fig. 3. Effect of initial molasses concentration on adsorption capacity: filled data points for fresh adsorbent and open data points for regenerated adsorbent.

Fig. 3 depicts the adsorption capacity of the adsorbent with respect to contact time. The filled and open data points represent the fresh and regenerated adsorbents, respectively. As observed in this figure, increasing the initial molasses concentration from 6 to 12 g/*l* improved the adsorption capacity from 98 to 170 mg/g. This increase was due to the great driving force provided by high molasses concentrations to overcome the mass transfer resistance between the aqueous and solid phases. A similar trend was followed while using the regenerated adsorbents. The adsorption capacity of the regenerated adsorbents was slightly different from the fresh ones, which confirmed the effectiveness of the regeneration process. The obtained results demonstrated that after a contact time of 7 h, a molasses removal efficiency of 82, 78, 75 and 74% was achieved for initial concentrations of 6, 8, 10 and 12 g/*l*, respectively.

2. Adsorption Isotherm

Adsorption isotherms are used to evaluate the performance of the adsorbents in the adsorption process. They represent the surface properties of the adsorbents and also describe the interaction

Table 3. The constants and important parameters of various applied isotherms

Isotherm	Parameters	Obtained values
Langmuir	q_{max}	210.54
	K_L	2.273×10^{-4}
	R^2	0.881
	Δq (%)	17.641
Freundlich	K_F	1.352
	n	1.642
	R^2	0.975
	Δq (%)	4.440
Temkin	B_1	84.37
	K_T	2.736
	R^2	0.937
	Δq (%)	6.258
Harkins-Jura	B_2	3.687
	A	6250
	R^2	0.980
	Δq (%)	3.232

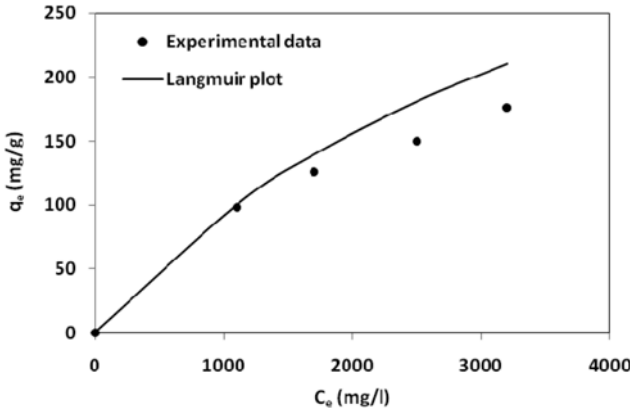

Fig. 4. Langmuir adsorption isotherm fitted to the experimental data.

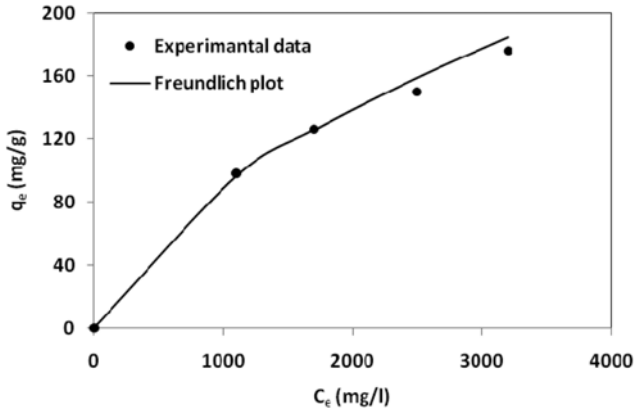

Fig. 5. Freundlich adsorption isotherm fitted to the experimental data.

between the adsorbate and adsorbent [26,27]. Various adsorption isotherms were applied in this study to fit the experimental data. The results of this investigation are in Table 3. The constant and coefficients of the adsorption models were calculated from the linear plot of the isotherms. The suitability of the applied adsorption isotherm to represent the experimental data was verified in terms of regression coefficient (R^2). Generally, the regression coefficient is not a sufficient criterion for selection of a suitable model. Thus, a normalized standard deviation (q) was used to compare the validity of the models [18,28]:

$$(\Delta q)\% = \sqrt{\frac{\sum[(q_{exp} - q_{cal})/q_{exp}]^2}{N-1}} \times 100 \quad (3)$$

where N is the number of data points. The higher value of R^2 and lower value of q implies the accuracy of a model to predict the experimental results. The obtained values of R^2 and Δq for the various adsorption isotherms are in Table 3.

Fig. 4 shows the Langmuir equation fitted to the experimental data. The Langmuir isotherm represents the monolayer coverage of the adsorbate on the adsorbent surface. As observed in this figure, the Langmuir model failed to fit the experimental data, and thus the adsorption of the molasses on the adsorbent surface was not monolayer. The calculated R^2 (0.881) and Δq (17.641) also confirm the deviation of this model from the experimental results. Generally, a dimensionless equilibrium parameter (R_L), which is also known as a separating factor, is used to assess the Langmuir isotherm. R_L is represented by the following equation:

$$R_L = \frac{1}{(1 + K_L C_0)} \quad (3)$$

where C_o is the initial solute concentration and K_L is the Langmuir constant. The value of R_L>1 represents unfavorable, R_L=1 linear, 0<R_L<1 favorable and R_L=0 irreversible adsorption process [29]. In the current work, the R_L values of 0.423, 0.355, 0.306 and 0.268 were, respectively, obtained for molasses concentrations of 6, 8, 10 and 12 g/*l*, which indicates a favorable adsorption process.

The Freundlich isotherm is usually applied to predict the surface heterogeneity of the adsorbent as well as multilayer coverage on the surface. The Freundlich isotherm applied to the experimental data is depicted in Fig. 5. It was observed that the achieved experimental data were well represented by the Freundlich isotherm with R^2 of 0.975 and a corresponding Δq value of 4.44. The coefficients of K_F and n were easily obtained from the intercept and slope of the linearized isotherms (Table 3). The magnitude of n gives an idea about the favorability of the adsorption process and n>1 indicates favorable adsorption condition [30]. In the current investigation, an n value of 1.642 was obtained, which satisfies the favorable criterion.

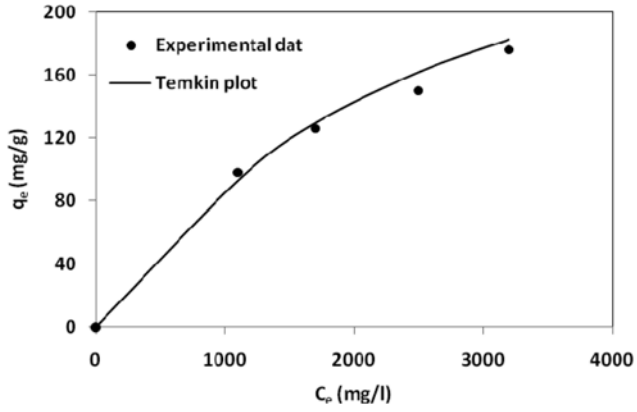

Fig. 6. Temkin adsorption isotherm fitted to the experimental data.

The Temkin isotherm assumes uniform distribution of binding sites on the adsorbent surface. Fig. 6 represents the plot of this isotherm applied to the experimental data. The values of Temkin rate constant (K_T) and B_1 determined from the slope and intercept of the linearized isotherms are in Table 3. The obtained results revealed that this model was fairly well fitted to the experimental data due to the achieved values of R^2 (0.937) and Δq (6.258).

The Harkins-Jura adsorption isotherm was also applied to predict the adsorption behavior of the system as presented in Fig. 6. The constants of the isotherm were calculated from the slope and intercept of the linearized isotherm (Table 3). Amongst the various adsorption isotherms, this model showed a good agreement with the obtained experimental data with R^2 of 0.980 and Δq of 3.233. The Harkins-Jura adsorption isotherm represents the existence of heterogeneous pore distribution in the structure of adsorbent and indicates multilayer adsorption of adsorbate on the surface.

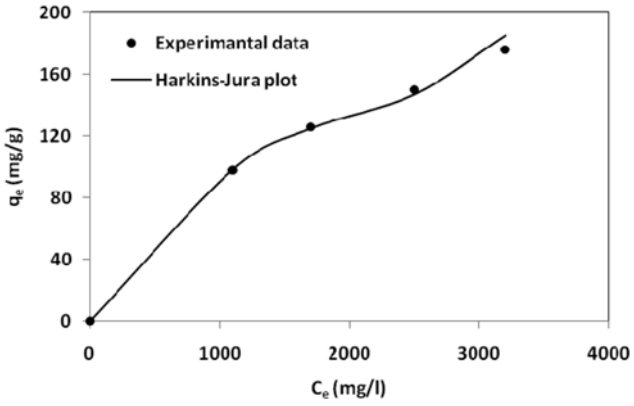

Fig. 7. Harkins-Jura adsorption isotherm fitted to the experimental data.

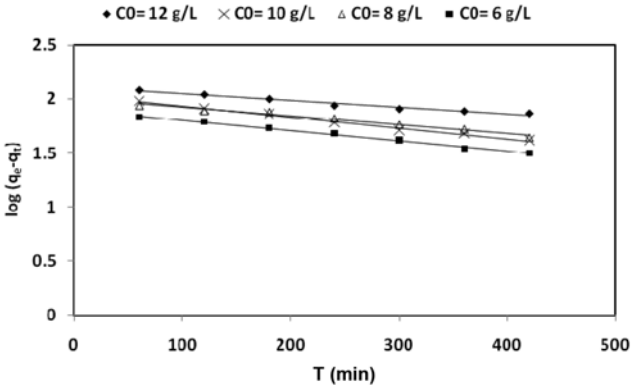

Fig. 8. The linearized form of the pseudo-first order kinetic model.

3. Kinetic Studies

Kinetic models have been proposed to determine the mechanism of the adsorption. The adsorption mechanism depends on the physical and chemical properties of the adsorbent and also the mass transfer process [27]. In the present investigation, various kinetic models

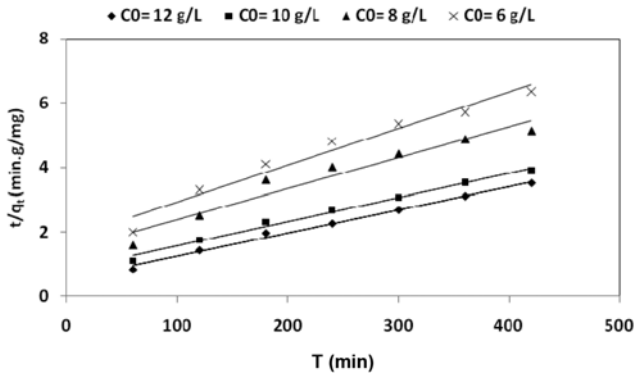

Fig. 9. The linearized form of the pseudo-second order kinetic model.

were applied to the obtained experimental data. The pseudo-first order kinetic model in the linearized form which is a plot of log (q_e−q) against t is presented in Fig. 8. The rate constant of k_1 was determined from the slope of the plot (Table 4). It was observed that the obtained experimental data were in a good agreement with this model, and a high correlation coefficient of $R^2 \geq 0.970$ was obtained in all cases. However, the calculated q_e values showed a great deviation from the experimental ones, which demonstrates the inapplicability of this model to describe the kinetics of molasses adsorption on the adsorbent.

Fig. 9 shows the linearized form of the pseudo-second order model applied to the experimental data. The calculated kinetic parameter of the model is also presented in Table 4. It was observed that the achieved experimental data were in a very good agreement with this kinetic model especially at high molasses concentrations (R^2=0.99). Besides, in most cases the calculated values of q_e which were obtained from this model were in a reasonable agreement with the experimental data. Such agreements between the calculated parameters and experimental data imply that the adsorption of molasses on the adsorbent follows pseudo-second order kinetic model.

The Elovich kinetic model is usually used to describe the chemi-

Table 4. The kinetic parameters of various applied kinetic models

Kinetic model	Parameters	Obtained values			
		C_0=12	C_0=10	C_0=8	C_0=6
Pseudo-first order	k_1	2.303×10^{-4}	2.303×10^{-3}	4.606×10^{-4}	2.303×10^{-4}
	q_{cal}	127.938	107.646	100.231	76.067
	q_{exp}	170.232	150.816	126.312	98.534
	R^2	0.970	0.991	0.975	0.993
Pseudo-second order	k_2	9.298×10^{-5}	6.044×10^{-5}	5.716×10^{-5}	6.794×10^{-5}
	q_e	166.667	142.857	111.111	90.909
	q_{exp}	170.232	150.816	126.312	98.534
	R^2	0.992	0.990	0.941	0.964
Elovich	α	109.563	284.777	282.906	359.427
	β	0.039	0.035	0.046	0.052
	R^2	0.973	0.983	0.912	0.946
Intra-particle diffusion	K_i	3.940	4.319	3.405	2.960
	I	41.51	21.01	9.22	5.14
	R^2	0.985	0.994	0.969	0.990

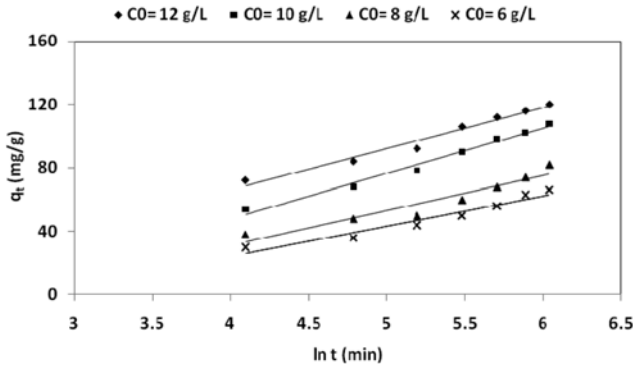

Fig. 10. The linearized form of the Elovich kinetic model.

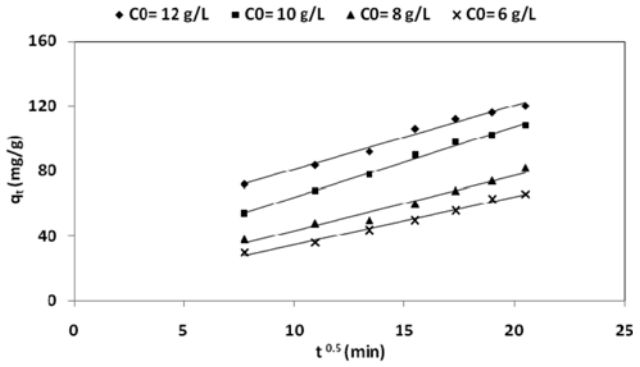

Fig. 11. The linearized form of the intra-particle diffusion model.

sorptions of adsorbate on the adsorbent with a heterogeneous surface [18]. Fig. 10 presents the linearized form of the Elovich kinetic model. The slope and intercept of a plot of q against ln t were used to calculate the model constants as shown is Table 4. This model also presented a relatively good agreement with the achieved experimental data.

The intra-particle diffusion model was also implemented to identify the diffusion mechanism of the adsorbate and the rate-controlling step. Generally, sorption of adsorbate on adsorbent includes several steps of i) transport of the solute molecule from the bulk aqueous phase to the adsorbent surface, which is considered as film diffusion, and ii) diffusion of the adsorbate into the interior structure of the adsorbent [31]. The intra-particle diffusion gives an insight to the diffusion mechanism. The linear form of this kinetic model is depicted in Fig. 11, which is a plot of q against $t^{0.5}$. The intra-particular diffusion rate constant was obtained from the slope of this plot (Table 4). Also, the value of I (intercept) gives an idea about the thickness of the boundary layer and the large values of I represent great effect of boundary layer [32]. It was concluded that the diffusion was the rate-controlling step due to the considerable values obtained for I and good agreement of the experimental data with this kinetic model at various molasses concentrations (Table 4).

CONCLUSION

Removal of melanoidin pigment from molasses spent wash was investigated by using a novel fabricated adsorbent. The achieved equilibrium data were analyzed through various adsorption isotherm models. The obtained experimental data were well described by Harkins-Jura and Freundlich isotherms which represent the multilayer adsorption and heterogeneous surface of the adsorbent. Among various kinetic models applied to the experimental data, the best fit was obtained with a pseudo-second order kinetic model. Also, the adsorption mechanism was successfully predicted using the intra-particle diffusion model. It was also concluded that the decolorization process did not influence the sugar concentration of the molasses solution.

ACKNOWLEDGEMENT

The authors gratefully acknowledge the research committee of Noushirvani University of Technology, for the support and facilities provided in the Biotechnology research lab.

NOMENCLATURE

C_e : equilibrium concentration of adsorbate in the solution [mg/*l*]
C_o : initial concentration of adsorbate in the solution [mg/*l*]
q_e : amount of adsorbate per mass of adsorbent at equilibrium [mg/g]
q_{max} : maximum adsorption capacity of the adsorbent [mg/g]
q_t : amount of adsorbate per mass of adsorbent at time t [mg/g]
K_L : Langmuir adsorption constant [*l*/mg]
K_F : Freundlich adsorption constant [(mg/g)·(l/g)$^{1/n}$]
n : dimensionless adsorption intensity in Freundlich equation
K_T : Temkin equilibrium binding constant [*l*/mg]
B_1 : Temkin adsorption constant
t : time [min]
A : Harkins-Jura adsorption constant [mg^2/g·*l*]
B_2 : Harkins-Jura adsorption constant [g/*l*]
k_1 : pseudo-first order adsorption rate constant [1/min]
k_2 : pseudo-second order adsorption rate constant [g/mg·min]
K_i : Intra-particular diffusion rate [mg/g·min$^{0.5}$]
I : constant related to the thickness of boundary layer
r_p : adsorbent particle radius [m]
D : effective diffusivity of adsorbate within the adsorbent [m^2/min]
V : volume of molasses solution [*l*]
W : mass of the adsorbents [g]
α : Elovich initial adsorption rate constant [mg/g·h]
B : Elovich constant related to the extent of surface coverage and activation energy g/mg]

REFERENCES

1. J. Escobar, E. Lora, O. Venturini, E. Yáñez, E. Castillo and O. Almazan, *Renewable Sustainable Energy Rev.*, **13**, 1275 (2009).
2. R. Saxena, D. Adhikari and H. Goyal, *Renewable Sustainable Energy Rev.*, **13**, 167 (2009).
3. A. Demirbas, *Prog. Energy Combust. Sci.*, **33**, 1 (2007).
4. K. Hatano, S. Kikuchi, Y. Nakamura, H. Sakamoto, M. Takigami and Y. Kojima, *Bioresour. Technol.*, **100**, 4697 (2009).
5. H. Adikane, M. Dange and K. Selvakumari, *Bioresour. Technol.*, **97**, 2131 (2006).
6. S. Sirianuntapiboon, P. Phothilangka and S. Ohmomo, *Bioresour.*

Technol., **92**, 31 (2004).
7. S. Sirianuntapiboon, P. Zohsalam and S. Ohmomo, *Process Biochem.*, **39**, 917 (2004).
8. C. Raghukumar, C. Mohandass, S. Kamat and M. Shailaja, *Enzyme Microb. Technol.*, **35**, 197 (2004).
9. Y. Zeng, Z. Liu and Z. Qin, *J. Hazard. Mater.*, **162**, 682 (2009).
10. H. Mudoga, H. Yucel and N. Kincal, *Bioresour. Technol.*, **99**, 3528 (2008).
11. R. Chandra, R. Bharagava and V. Rai, *Bioresour. Technol.*, **99**, 4648 (2008).
12. R. Krishna Prasad and S. Srivastava, *J. Hazard. Mater.*, **161**, 1313 (2009).
13. T. Tondee, S. Sirianuntapiboon and S. Ohmomo, *Bioresour. Technol.*, **99**, 5511 (2008).
14. T. Tondee and S. Sirianuntapiboon, *Bioresour. Technol.*, **99**, 6258 (2008).
15. R. Krishna Prasad and S. Srivastava, *Chem. Eng. J.*, **146**, 90 (2009).
16. T. Nandy, S. Shastry and S. Kaul, *J. Environ. Manage.*, **65**, 25 (2002).
17. P. Sohsalam and S. Sirianuntapiboon, *Bioresour. Technol.*, **99**, 5610 (2008).
18. S. Figaro, J. Avril, F. Brouers, A. Ouensanga and S. Gaspard, *J. Hazard. Mater.*, **161**, 649 (2009).
19. S. Figaro, S. Louisy-Louis, J. Lambert, J. Ehrhardt, A. Ouensanga and S. Gaspard, *Water Res.*, **40**, 3456 (2006).
20. N. Öztürk and D. Kavak, *J. Hazard. Mater.*, **127**, 81 (2005).
21. L. Thomas, G. Chamberlin and G. Shute. *Colorimetric chemical analytical methods: Tintometer*, New York (1980).
22. M. Robert, R. M. Silverstein, G. C. Bassler and T. C. Morrill, *Spectrometric identification of organic compounds*, John Wiley & Sons Inc, New York (1991).
23. M. El-Halwany, *Desalination*, 208 (2009).
24. N. K. Amin, *J. Hazard. Mater.*, **165**, 52 (2009).
25. M. Zhao and P. Liu, *Desalination*, **249**, 331 (2009).
26. M. Ugurlu, *Micropor. Mesopor. Mater.*, **119**, 276 (2009).
27. D. Özer, G. Dursun and A. Özer, *J. Hazard. Mater.*, **144**, 171 (2007).
28. M. Mondal, *Korean J. Chem. Eng.*, **27**, 144 (2010).
29. A. Franca, L. Oliveira and M. Ferreira, *Desalination*, **249**, 267 (2009).
30. G. Kumar, P. Ramalingam, M. Kim, C. Yoo and M. Kumar, *Korean J. Chem. Eng.*, In press.
31. P. Monash and G. Pugazhenthi, *Korean J. Chem. Eng.*, **27**, 1 (2010).
32. R. Ahmad, *J. Hazard. Mater.*, **171**, 767 (2009).